ELSEVIER

Ceramics International 25 (1999) 107–113

CERAMICS INTERNATIONAL

Adsorption, rheology, packing, and sintering of nanosize ceramic powders

Dean-Mo Liu[1]

Materials Research Laboratories, Industrial Technology Research Institute, Chutung, Hsinchu, Taiwan 31015

Received 26 August 1997; accepted 8 January 1998

Abstract

Nanosize zirconia particles stabilised with a water-soluble polyelectrolyte in an aqueous medium were characterised in terms of adsorption behaviour, suspension rheology, and subsequent green/sintered compact microstructure. A monolayer surface coverage of the particle by adsorption was experimentally verified. The thickness of the adsorbed polyelectrolyte onto the powder particles was calculated to be 6.2 nm, which increases the "bare" particles by 14.6% in size. This adsorption increases the effective solid loading by as large as 51%. Rheological behaviour of the suspensions was experimentally determined which was well-described by an exponential function up to solid fractions of 20 vol%. The particle packing efficiency in the green consolidates appears to be solid-loading dependent; the higher the solid loading, the better the particle packing efficiency can be achieved. Green density as good as 52% theoretical can be obtained in suspensions containing 40% solid loading in this study. The sintered ceramic with an ultrafine microstructure of as fine as 0.14 μm in average grain size is obtained.

1. Introduction

Colloidal processing has long been recognised as a technologically important route of green-shape forming technique for advanced ceramic powders. A recent publication by Lange [1] has particularly emphasised the significance of colloidal filtration on the improved reliability of ceramic parts. The dispersion of ceramic powders in liquid media plays an important role in determining the resulting particle packing efficiency and final structure integrity and microstructure homogeneity after high-temperature densification. In an effort to obtain well dispersed powders, dispersing agents are most-frequently utilised either in aqueous or non-aqueous media. The powder particles are able to be stabilized either electrostatically (i.e., by electrolytes) or sterically (by polymers), or a combination of both (by polyelectrolytes). The use of water-soluble polyelectrolytes has been received great attention for many years in colloidal processing for fine ceramics not only ascribed to the advantages in dispersion control but also to the ecological requirements [2–4]. In this investigation, a water-soluble polyelectrolyte was used to disperse zirconia powder with nanosize particles in water. The rheological behaviour of the suspensions and resulting particle packing efficiency and densification of the powders are the focus of this investigation.

The rheological behaviour of nanosize (generally $<$ 100 nm) ceramic powders in polyelectrolyte-stabilised aqueous media has not yet been extensively reported. One possible reason may be due to their extensive agglomeration, particularly when the particle size is as small as a few nanometers, and this usually makes a clear illustration of suspension rheology more difficult and physically meaningless. This is therefore one of the reasons for this investigation to be performed and in order to avoid the difficulty in de-agglomeration of the nanopowder, a ceramic nanopowder, which was specifically prepared, containing almost free of agglomerates, is employed.

In view of the literature, a number of factors such as molecular weight and molecular structure of the polymer, charging effect, level of ionic strength, electroviscous effect, degree of adsorption, thickness of adsorbed layer, etc., have been realised to affect the rheology of the polyelectrolyte-stabilised suspensions in a wide variety of manners [2,5–8]. Theoretical considerations, although have taken some of the factors as

[1]Present address: Department of Materials Science and Engineering, University of Pennsylvania, 3231 Walnut Street, Philadelphia, PA 19104, USA.

0272-8842/99/$—see front matter
PII: S0272-8842(98)00009-1

primary considerations, have their respective limitations in prediction, particularly for suspensions with lower solid fractions. One of the well-known models is proposed by Mooney [9] who described suspension rheology as an exponential function which has a general formula

$$\eta = \exp\left(\frac{\alpha\phi_o f}{1 - kf\phi_o\lambda}\right) \quad (1)$$

where η is the relative viscosity of the suspension at infinite shear rate, $\alpha = 2.5$ for rigid uncharged spherical particles, ϕ_o is the particle volume fraction, λ is the polydispersity factor and is equal to unity for monodisperse systems, k is the clowding factor, and f is a factor due to polymer adsorption which is a ratio of ϕ/ϕ_o, where ϕ is total volume fraction. Eq. (1) is generally involved a number of critical factors in dominating suspension rheology and is the primary model to be used in describing the rheological behaviour of the suspensions presently prepared. In a limiting case for dilute suspensions with rigid, uncharged spherical particles, Eq. (1) can be reduced to the well-known Einstein's equation [10], i.e., $\eta = 1 + 2.5\,\phi_o$.

The particle packing efficiency of nanopowders is an important subject of considerable interest for many researchers, primarily because ceramics with nano-scale microstructure exhibit unique physical properties such as hardness and electronic conductivity in comparison to those with submicro/micro-scale microstructures [11]. Recently, a number of publications have reported to obtain high-density green nanopowder compacts via ultrahigh compressive pressure [12,13]. The relatively large interparticle friction of the nanosized particles restricts particle movement which enhances difficulty in reaching higher packing efficiency, resulting in a lower green density. Moreover, microstructural inhomogeneity such as coarse grain/pore, can usually result during the course of final sintering stage. In contrast, a better microstructure integrity and homogeneity can generally be obtained via colloidal filtration [1,14,15]. In this study, the particle packing efficiency of the green compacts was characterised in terms of green density and pore size distribution. The green and sintered microstructures of the compacts were also examined microscopically.

2. Experimental procedures

Aqueous suspensions containing 5–40 vol% nanosize (average particle size = 85 nm) powders and 3.38 wt% (on powder basis) polyelectrolyte dispersant (having an average molecular weight = 5000). This quantity of the dispersant is sufficiently enough to reach a complete surface coverage under pH 6.5 based on our previous work [16]. High-purity 3 mol% Y_2O_3-stabilised zirconia ceramic powders with impurity content (e.g., CaO, Al_2O_3, TiO_2, and Fe_2O_3) less than 0.05% was used. This powder was dispersed in deionized, distilled water and the suspension pH was adjusted using analytical-grade ammonia water and HCl acid. The suspensions were prepared using a ball milling with high-purity zirconia grinding balls for 24 h. After degassing, the suspensions were cast onto a plaster mold to form green compacts. Adsorption test was performed by separation of the solid phase from solution (supernatant) via centrifugation. The solid phase was washed several times with sufficient amount of deionized water to ensure no excess polymer being deposited (other than those being absorbed) onto the particle surface. The adsorbed polymer was then determined using a thermal gravimetric analyser (TGA, Netzsch, Model 402) to an accuracy of $\pm$ 0.01 mg.

The particle size distribution of the powder was examined using a particle size analyser (Horiba A930). The green density together with the pore size distribution of the green compacts are characterised using a pore size analyser (Autopore 9220). Four to six specimens are used to determine the mean green density for a given suspension and there is an experimental error of 0.67%. The average pore size (i.e., $4V/S$), where V represents the pore volume and S the pore surface area, is used as a representation for the whole spectrum of pores within the green compacts and has an experimental error within 1% among the test specimens. A cone-and-plate viscometer (Brookfield) was used to measure the viscosity of the suspensions (η_s) and the supernatant (η_o) over shear rate ranging from 0.7 to 300 s^{-1}. The relative viscosity (η) as defined in Eq. (1) of the suspensions is determined as the ratio of suspension viscosity to supernatant viscosity at infinite shear rate. The green and sintered microstructure of the nanoceramic were measured using a scanning electron microscopy (SEM, Cambridge Instruments, S-360).

3. Results and discussion

3.1. Powder characterisation

Fig. 1 shows the morphology of the powders. The particles generally show almost an equiaxial geometry with aspect ratio of approximately 1–1.12. The particles can be considered, as a rough approximation, to be spherical in shape and have an average diameter of approximately 85 nm. Some particle clusters are apparently present which are indicative of the presence of agglomerates. The particle size (d) determined using the B.E.T. nitrogen adsorption method is about 60 nm ($d = 6/\rho \times S$, where ρ is the theoretical density of the solid and S, the specific surface area of the powder, 16.4 $m^2\,g^{-1}$). The difference between the BET-deter-

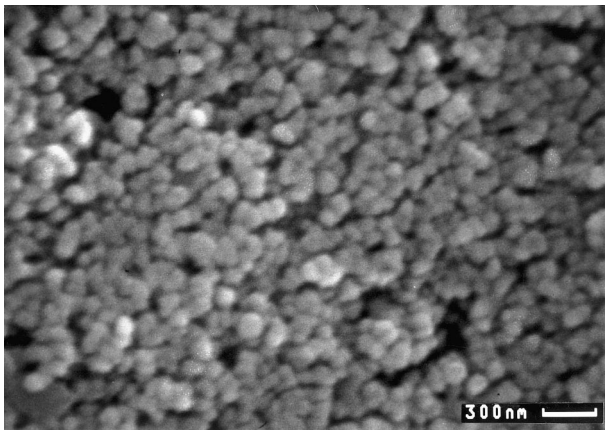

Fig. 1. Nanopowder morphology.

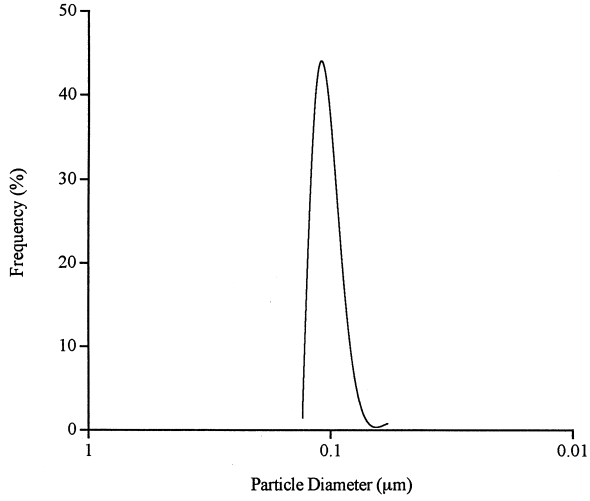

Fig. 2. Particle size distribution of the nanosize powder.

mined and microscopically-measured particle size may be due to the presence of intraagglomerate porosity, which is accessible to nitrogen, resulting in an increase in specific surface area, which reduces *d*. The particle size distribution of the powder is shown in Fig. 2 The particles distribute over a relatively small range of size from 0.06 to 0.15 μm, which is essentially a unimodal character. The larger particles, e.g., 0.15 μm in diameter, in size distribution suggests the presence of some levels of agglomeration, which is also consistent with the particle size microscopically observed.

3.2. Adsorption behaviour

In a previous study [16], the present author has demonstrated that the adsorption of the water-soluble polyeletrolyte onto nanosize zirconia powders is strongly dependent on solution pH and a pH of 6.5 together with sufficient amount of the polyelectrolyte as currently controlled ensure a complete monolayer surface coverage. The adsorbed polymer onto the powder surface was measured for all the prepared suspensions and has an average value of $0.54\,mg\,m^{-2}$ with a standard deviation of $0.02\,mg\,m^2$. This adsorbed amount determined presently is almost identical with that measured previously at this pH range and is suggestive of a saturation adsorption being attained. The particles are therefore in a good dispersing condition as can be verified in Fig. 2. If, as theoretically expected, the particle surface was completely covered with a layer of polymer, then the effective surface area for a molecule of the polymer to be covered can be calculated through the powder specific surface area and adsorbed amount experimentally determined, which yields a value of approximately $1550\,Å^2$. This value is generally in reasonable agreement with the value commonly used in the literature, for instance, over a range of 1000–$2000\,Å^2$. The thickness of the adsorbed layer by the polyelectrolyte, which is an important parameter for a fundamental characterisation of adsorption behaviour, is determined through the use of rheological data of the suspensions and will be discussed in the following section.

3.3. Rheological behaviour

Eq. (1) has readily been used correctly in describing the rheological behaviour of a number of simple suspension systems, particularly for uncharged, spherical particles, over a finite suspension concentrations [17]. Before a further calculation can be conducted, it is reasonably to assume that the polydispersity factor λ is equal to unity based on the particle size distribution revealed in Fig. 2 and Eq. (1) can then be rewritten as

$$\eta = \exp\left(\frac{\alpha\phi_o f}{1 - k\phi_o f}\right) \tag{2}$$

After rearrangement and expressing in a linear form;

$$\frac{\phi_o}{ln\,\eta} = \frac{1}{\alpha f} - \frac{k\phi_o}{\alpha} \tag{3}$$

The viscosity for both the suspension (η_s) and corresponding supernatant (η_o) can be determined using a viscosity–(shear rate)$^{-1/2}$ plot, following by extrapolating the curve to the value at which (shear rate)$^{-1/2} = 0$, i.e., infinite shear rate. Fig. 3 show one of the plots for 30 vol% suspension. The intrinsic relative ($\eta = \eta_s/\eta_o$h) can then be obtained for each suspension.

Substituting the obtained η together with the particle solid fraction ϕ_o into Eq. (3), a plot of ϕ_o/ln η vs ϕ_o should yield a straight line with the slope identical to the ratio of k/α and the intercept equal to the inverse of (α *f*). As expected, a straight line appears to be

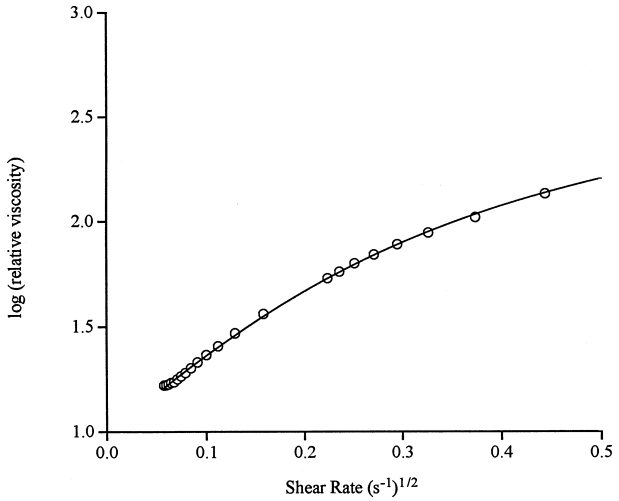

Fig. 3. Relative viscosity vs (shear rate)-1/2 for 30% loading suspension.

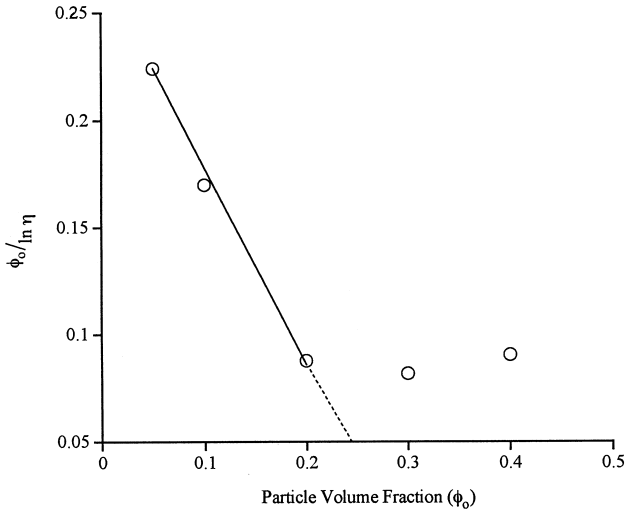

Fig. 4. A plot of $\phi_o/\ln \eta$h vs ϕ_o shows a linearity up to solid fractions of 20%.

well-correlated with the solid loading up to 20 vol% (Fig. 4). Considerable deviation between experimentally-determined and model-predicted values occur when solids loading greater than 20%. One possible explanation for such deviation may arise from a greater supernatant viscosity η_o due to higher residual polymer concentration in corresponding supernatant, which causes a reduction in ln η, resulting in a greater value of $\phi_o/\ln \eta$. However, the actual reason is unclear at present Therefore, in order to have a physically meaningful correlation on suspension rheology with theoretical expectation, attention will be focused on the suspensions with solid fractions $\leq 20\%$.

After determination of the slope and intercept from the straight line in Fig. 4, the ratio of k/α and the inverse of (αf) can then be calculated with an assumed $\alpha = 2.5$. The rheological behaviour of the suspensions can then be expressed in a more quantitative form of

$$\eta = \exp\left(\frac{3.77\phi_o}{1 - 3.38\phi_o}\right) \tag{4}$$

By substituting the particle volume fraction (ϕ_o) into Eq. (4), Fig. 5 illustrates the resulting predicted (solid) curve with the experimental data (open circles). Obviously, the prediction is well consistent with experimental results at solid fractions $\leq 20\%$ as originally expected in Fig. 4. The use of $\alpha = 2.5$ in estimate of Eq. (4) appears to be valid, even though it was originally derived for uncharged spherical particles. Nevertheless, differences in inter-particle properties (particularly inter-particle potential) in the suspensions presently prepared and those theoretically proposed (here termed "model" suspension) by Einstein are significant, e.g.,

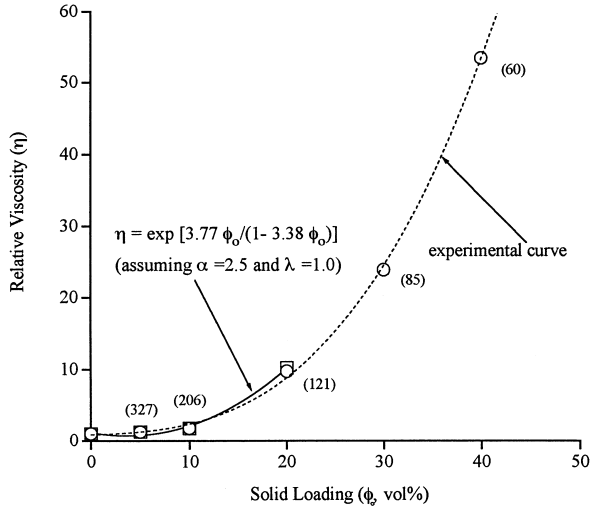

Fig. 5. Relative viscosity of the suspension for differing solids loading along with the model-predicted viscosity, both agrees with solid fraction up to 20%.

charged vs uncharged particles, concentrated vs dilute suspension. Strictly speaking, electroviscous effect due to the presence of the charged particles may arise and it would change the α value in different extents [18]. However, a detailed analysis on this subject is not the prime focus of the present investigation. Instead, the consistency of suspension rheology between the experimental results and predicted values (Fig. 5) implies the presence of some similarity in inter-particle potential, although can hardly be quantified presently, between both types of suspension. In other words, we believe that such potential similarity in respective suspension is responsible for the nearly identical rheology.

Since inter-particle potential is a strong function of inter-particle separation, estimate of the separation may provide some clues for a better understanding on such similarity. The inter-particle separation is estimated using the model derived statistically by Ashby et al. [19] and is indicated in the parentheses in Fig. 5 for the suspensions. Accordingly, the separation for 20% loading is 121 nm which is believed to be a hydrodynamically "safe" distance that minimises possible interactions such as van der Waals attractive force (having generally an effective separation of up to 30–40 nm) and so-called hydrophobic force, up to 70–80 nm [20]). A further increase in the separation, for instance, in the case of 5 or 10% loading suspension, the inter-particle interactions may be markedly reduced to a negligible level. In other words, we hypothesise that the particles may behave, to some extent, independently with respect to each other in the suspensions as those in the "model" suspension. If this assumption is sustained, then the use of $\alpha = 2.5$ is permitting without causing considerably quantitative error in prediction as readily illustrated in Fig. 5. In fact, this may be particularly true when the shear rate is approaching infinite as a previous determination of η. However, such interactions should not be ignored when the solid fraction is high enough, e.g., greater than 30%, where inter-particle separation is relatively small, even under the condition of intensive shear field. In the derivation of Eq. (4), the factor f (i.e., ϕ/ϕ_o) due to polymer adsorption onto the particles was obtained to have a value of 1.51. This adsorption changes the "bare" particle diameter (d) by a layer a polymer with a thickness (δ) which can be estimated using [21]

$$f = \left(1 + \frac{2\delta}{d}\right)^3 \tag{5}$$

After calculation, the hydrodynamic thickness (δ) of the adsorbed polymer is 6.2 nm, having a magnitude of 7.3% of the "bare" particle diameter, which is in reasonable agreement with the literature report for polyelectrolyte adsorption [6]. This adsorption layer increases the total solid fraction in the suspensions by as large as 51%.

The hydrodynamic size of the particles is increased due to polyelectrolyte adsorption. This results in a decrease in inter-particle separation, for instance, 121 nm→109 nm for 20% suspensions and 85 nm→73 nm for 30% suspension, etc. Nevertheless, in spite of the decrease in the separation, the current experimental results suggest that the "corrected" separation in 20% suspension may still be a "safe" hydrodynamic distance permitting a good prediction by the analytical equation.

3.4. Packing and densification

The particle packing configuration of the green compacts consolidated from suspensions was examined in terms of pore size distribution and packing structure by direct SEM observation. Fig. 6 illustrates the pore distribution of the compacts made from suspensions of different solid fractions. The pore size distribution for 5 and 20% compacts has roughly identical characteristic, suggesting considerable similarity in particle packing configuration, and becomes finer in pore size at 30% and further at 40% compacts. These indicate a better packing efficiency can be achieved by using concentrated suspensions. Although the dispersion characteristic of the powder particles appears to be similar from previous observation, the resulting pore distribution suggests that such similarity may not be entirely accounted for subsequent consolidation behaviour. The rate of liquid drainage, a decreasing particle mobility and separation in the suspension accompanied with stronger inter-particle interaction during liquid drainage may affect resulting packing configuration. This may particularly be true for dilute suspensions. In contrast, for concentrated suspensions the particles are restricted to or "locked" in a limiting space until consolidation is completed. The originally relative particle coordination with each other in the suspension may thus be retained to a significant extent after consolidation. That is to say, for concentrated suspensions, the resulting particle packing efficiency is strongly and directly dependent on the starting dispersion characteristic of the particles. The better the particles dispersed in concentrated suspension, the better the resulting particle packing efficiency can be expected.

The green density of the consolidates is inversely linearly correlated with the average pore size, as shown in

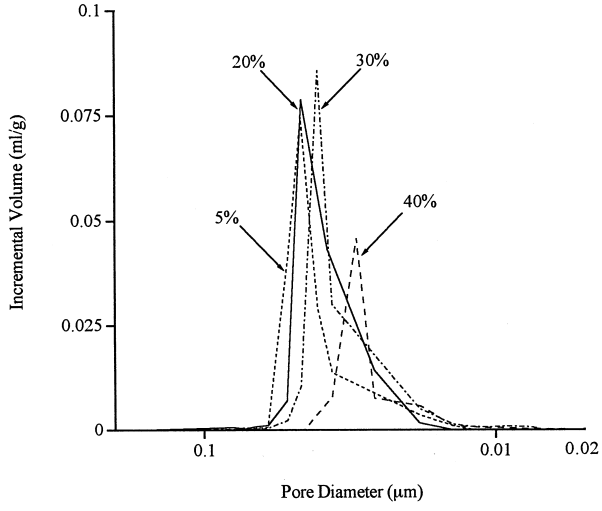

Fig. 6. Pore size distribution of the green powder compacts made from suspensions of varying solid fractions.

Fig. 7 with the solid fractions indicate in the parentheses. The use of average pore size is due to its sensitive nature to the variation in pore size distribution and has been confirmed in previous publications [21,22]. In current investigation, the green density as good as about 52% theoretical is obtained for 40% suspension.

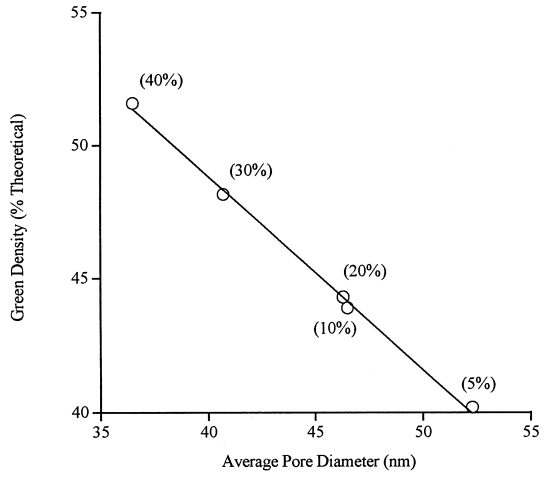

Fig. 7. Green density of the powder compacts as an inversely linear function of the average pore diameter of the corresponding green compact.

Figs. 8(a) and (b) show the scanning electron micrographs of the packing microstructure for 5 and 40% suspensions. Obviously, a coarser pore structure is observed in 5% consolidate than that in 40% consolidate. This further verifies the pore distribution analysis illustrated in Fig. 6. After sintering at 1500°C, the corresponding sintered microstructure is shown in Figs. 9(a) and (b), respectively. Both sintered compacts have a density over 99.5% theoretical. The better packing efficiency (Fig. 8(b)) results in a finer grain microstructure (Fig. 9(b)), 0.14 μm in average, and coarser grain microstructure (Fig. 9(a)), i.e., 0.21 μm in average, for poorer particle packing compact (Fig. 8(a)). It is interesting to note that the sintered grains have a size larger by only 64.7% than the starting particle size. This increase in final grain size compared to the starting particle size is substantially smaller in magnitude than those reported in the literature, e.g., a magnification of particle-to-grain size over 10 times or even higher order was frequently observed, with starting particles of as small as a few nanometers in size [13]. This investigation therefore implies that a further reduction in sintered microstructure to, e.g. 100 nm-sized grains, is highly possible by optimisation of starting particle size and subsequent process control.

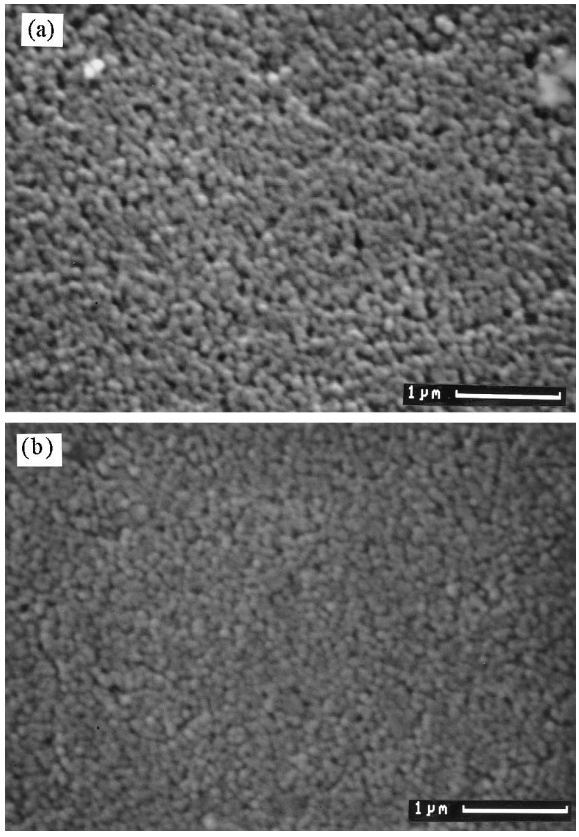

Fig. 8. Particle packing structure in the green zirconia compacts made from (a) 5% and (b) 40% loading suspensions.

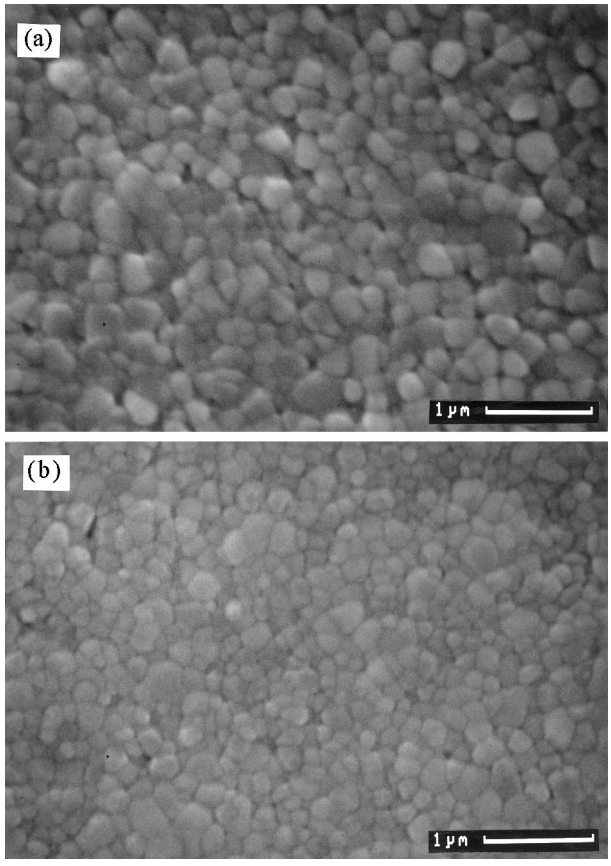

Fig. 9. Grain microstructure of the sintered compacts made from (a) 5% and (b) 40% loading suspensions.

4. Conclusion

The adsorption and rheological behaviour of nano-size zirconia powders were investigated in an aqueous medium. The particles were stabilised with a water-soluble polyelectrolyte by adsorption of a layer of polymer with 6.2 nm in thickness. This increase in hydrodynamic size of the particles causes an increase in solid fraction by as large as 51% in the suspensions. The rheological behaviour of the suspensions can be well described using a Mooney-type model, i.e., an exponential form, for solid loading up to 20%. The particle packing efficiency is improved for concentrated suspensions, e.g., 40%, and a green density as good as 52% theoretical can be easily obtained. Sintered compacts with nearly full density and ultrafine grain microstructure, 0.14 μm in average, can therefore be achieved via a simple sintering schedule after a proper colloidal processing control.

Acknowledgement

The author is gratefully indebted to the Minister of Economic Affair, Taiwan, for funding toward this work under contract no 873KG2220.

References

[1] F.F. Lange, Powder processing science and technology for increased reliability, J. Am. Ceram. Soc. 72 (1989) 3–15.
[2] J.A. Cesarano III, I.A. Aksay, Processing of highly concentrated aqueous α-alumina suspensions stabilized with polyelectrolytes, J. Am. Ceram. Soc. 71 (12) (1988) 1062–1067.
[3] H. Okamato, M. Hashiba, Y. Nurishi, K. Hiramatsu, Fluidity and dispersion of alumina suspension at the limit of thickening by ammonium polyacrylates, J. Mater. Sci. 26 (1991) 383–387.
[4] M. Hashiba, H. Okmato, Y. Nurishi, K. Hiramatsu, Dispersion of ZrO_2 particles in aqueous suspensions by ammonium polyacrylates, J. Mater. Sci. 24 (1989) 873–876.
[5] J. Cesarano III, I.A. Aksay, A. Bleier, Stability of α-alumina suspensions with poly(methacrylatic acid) polyelectrolytes, J. Am. Ceram. Soc. 74 (4) (1988) 250–255.
[6] J. Papenhuijzen, H.A. van der Schee, G.J. Fleer, Polyelectrolyte adsorption I, J. Colloid Interface Sci. 104 (2) (1985) 540–561.
[7] P.D. Patel, W.B. Russel, An experimental study of aqueous colloidal suspensions containing dissolved polymer, J. Colloid Interface Sci. 131 (1) (1989) 201.
[8] J. Mewis, A.J.B. Spaull, Rheology of concentrated dispersions, Adv. Colloid Interface Sci. 6 (1976) 173–200.
[9] M. J. Mooney, Colloid Sci. 6 (1951) 162.
[10] A. Einstein, Ann Physik. 19(4) (1906) 289.
[11] H. Gleiter, Materials with ultrafine microstructure: retrospectives and perspectives, Nanostruct. Mater. 1 (1992) 1–19.
[12] A. Pechenik, G.J. Piermarini, S.C. Danforth, Fabrication of transparent silicon nitride from nanosize particles, J. Am. Ceram. Soc. 75 (12) (1992) 3283–3288.
[13] J.R. Groza, R.J. Dowding, Nanoparticulate materials densification, Nanostruct. Mater. 7 (7) (1996) 749–768.
[14] I.A. Aksay, F.F. Lange, B.I. Davis, Uniformity of Al_2O_3–ZrO_2 composites by solloidal filtration, J. Am. Ceram. Soc. 66 (10) (1983) c190.
[15] I.A. Aksay, Microstructure control through colloidal consolidation, in: J. Mangels (Ed.), Advances in Ceramics, vol. 9, Forming of Ceramics, American Ceramic Society, Columbus, OH, 1984, pp. 94–104.
[16] D.M. Liu, Dispersion characteristic of nanosize zirconia powders in aqueous media, J. Mater. Sci. Letters (in press).
[17] J.W. Goodwin, The Rheology of Dispersions, Colloid Sci. 7 (1975) 246–293.
[18] B.E. Conway and A. Dobry-Duelaux, in F. Eirich (Ed.), Rheology, Theory, and Applications, vol. 3, Academic Press, New York, 1960, p. 83.
[19] G. Le Roy, J.D. Embury, G. Edward, M.F. Ashby, A model of ductile fracture based on the nucleation and growth of voids, Acta. Metall. 29 (1981) 1509–1522.
[20] H.K. Christenson, P.M. Claesson, Cavitation and the interaction between macroscopic hydrophobic surface, Science 239 (1988) 390–392.
[21] D.M. Liu, Influence of solid loading on the porosity evolution in ceramic injection moldings, J. Mater. Sci. (in press).
[22] D.M. Liu, C.T. Fu, Compaction behaviour of spray-dried silicon carbide powders, Ceramics International 22 (1966) 67–72.